Emission Intensity Dependence and Single-Exponential Behavior In Single Colloidal Quantum Dot Fluorescence Lifetimes

Brent R. Fisher, Hans-Jürgen Eisler, Nathan E. Stott, and Moungi G. Bawendi*

Department of Chemistry, Massachusetts Institute of Technology, Cambridge, Massachusetts 02139

Received: June 20, 2003; In Final Form: November 5, 2003

We present measurements of photoluminescence decay dynamics from single colloidal CdSe quantum dots. We find that the decays fluctuate in time with decay rates that correlate with time-averaged emission intensities. Moreover, the decays measured by selecting only those photons collected while the single quantum dot emission intensity was near its maximum yields single-exponential dynamics. We find that the "maximum-intensity" decays are nearly identical across different independently synthesized samples of nearly the same size. The combination of single-exponential kinetics and decays that are reproducible across samples leads us to speculate that it is the radiative lifetime that is measured and that the quantum yield of a single dot near its maximum emission intensity is close to unity. The variations in decay rates with time and their correlation with emission intensity indicate these intensity time trajectories primarily reflect fluctuations in nonradiative relaxation pathways.

Introduction

Since their initial development, interest in colloidal semiconductor nanocrystals or quantum dots (QDs) has largely centered on their unique optical properties. Excitons in a QD are quantum confined in all three dimensions, making optical properties like emission and absorption energies strongly size dependent. Many of the properties of colloidal QDs, when measured from an ensemble, can be masked by finite size distributions and by fluctuating local environments. Fortunately, the advent of these materials has closely followed the development of single chromophore optical microscopy and spectroscopy. These techniques have allowed the study of many QD optical properties without the blurring effects of size distribution. Moreover these techniques have led to the discovery of new phenomena in colloidal QD optical properties, such as blinking[1−3] and spectral diffusion,[4] that are not at all observed on the ensemble level.

The excited-state lifetime of colloidal QDs is one optical property that is not yet well understood. Photoluminescence (PL) decay dynamics of ensembles of colloidal QDs differ from those of traditional organic chromophores in two important ways. First, extremely long (tens of nanoseconds at room temperature to microseconds at low temperature) lifetimes are observed,[5] and second, the decays exhibit multiexponential dynamics. Three possible explanations for multiexponential behavior in the QD ensemble PL decay dynamics are: (i) each member of the ensemble has its own unique single-exponential (single-rate) lifetime, (ii) the PL decay is an inherently complex process for each individual QD, making the decay dynamics multiexponential for each member of the ensemble, or (iii) the PL decay of each member is single exponential at any given moment but it fluctuates in time, so that the time-averaged PL decay of an individual QD is multiexponential.

Single chromophore microscopy makes it possible to probe the nature of this multiexponential behavior on a dot-by-dot basis. Recent time-correlated single photon counting (TCSPC) experiments have shown that the PL decay from single CdSe colloidal QDs is in general multiexponential and, moreover, that the PL decay varies during the course of the TCSPC measurement.[6] The phenomenon of PL decay fluctuations has also been observed in single-molecule studies of organic and biological molecules,[7,8] but the multiexponential behavior seen in these studies is caused by fluctuations between different molecular conformational states, a parameter that is not present in the QD system. Instead fluctuations in the local electrostatic environment surrounding the QD should play an important role, as suggested in a study that correlated spectral diffusion with fluorescence blinking events in single QDs.[9] These electrostatic fluctuations may also lead to corresponding variations in the fluorescence quantum yield (QY) of each single QD. It was suggested that the QY of an ensemble of dots may represent an average over widely varying QY values from individual QDs;[10] time-dependent fluctuations would add a new dimension to this complex QY behavior.

The experiments presented here demonstrate that PL decay fluctuations from single colloidal CdSe QDs occur on time scales ranging at least up to many seconds. They confirm that PL decay rates are correlated to single QD time-averaged emission intensities. We also find that the ability to discriminate which photons are counted in TCSPC, for example by selecting only those photons emitted while the emission intensity is above a given threshold, can lead to single-exponential PL decays from single QDs. We propose that these single-exponential decays are a measurement of the radiative lifetime, thus providing a quantitative measure of the single-exponential radiative lifetime of colloidal CdSe QDs at room temperature.

Methods

Three different samples of ZnS-overcoated (4−5 monolayers) CdSe colloidal QDs were studied at room temperature. Each QD sample was synthesized independently using established methods[11] (see also Supporting Information). Overcoating was carried out using the methods of Dabbousi.[12] The samples had

* Author to whom correspondence may be addressed. E-mail: mgb@mit.edu.

10.1021/jp035756+ CCC: $27.50
Published on Web 12/06/2003

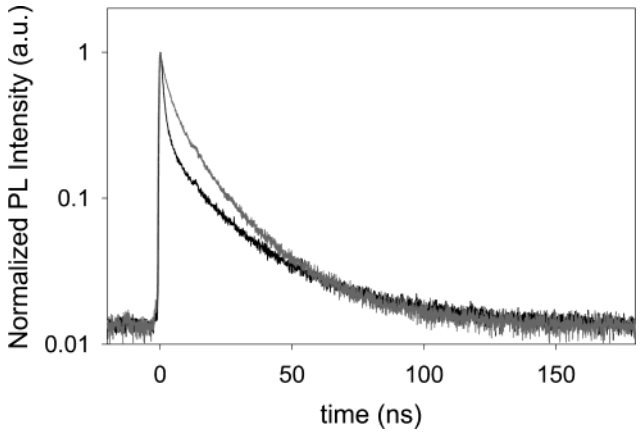

Figure 1. PL decays for two different single CdSe QDs (from sample 1) as measured by conventional TCSPC.

mean core radii of 3.1, 3.3, and 3.3 nm respectively. The samples were prepared for detection at the single-molecule level by spin casting (5000 rpm) a solution (~50 nM) of QDs in PMMA/toluene solution (200 mg/20 mL) onto a glass coverslip.

The experimental setup consisted of a home-built confocal scanning microscope with either 532- or 414-nm pulsed-laser excitation. The excitation laser light was focused through a pinhole and recollimated before entering the microscope. A dichroic mirror was used to couple the excitation light into the optical path, and galvanometer-driven scanning mirrors were used to generate scanned images of the single QDs. A 100*x* oil immersion objective (Nikon) with 1.25 NA was used to both focus the collimated laser and to collect the QD emission. Laser excitation at 532 nm with a pulse width of ~1 ps (Coherent MIRA-OPO) was provided by an intracavity frequency-doubled optical parametric oscillator (OPO) that was pumped by a Ti−Sapphire laser (MIRA) at 737 nm. A pulse picker was used to lower the OPO repetition rate to 4.75 MHz. Laser excitation at 414 nm was provided by a GaN diode-pumped laser with repetition rate of 5 MHz and pulse width of 90 ps (PDL800-LDH400, Picoquant, GmBH). An avalanche photodiode (APD, EG&G, SPCM-AQR14) was used for detection. Single photon counting was carried out using a time−digital converter integrated into a PC computer card (Timeharp 200, Picoquant GmBH).

Time-tagged, time-resolved (TTTR) measurements using the Timeharp were performed on each single quantum dot for a period of 120 or 180 s. TTTR measurements differ from traditional TCSPC in that both the start−stop time (time between excitation pulse and single photon emission, τ_p) and the absolute arrival time (time since the start of experiment, t_p) of each photon are measured. The resolution on τ_p was approximately 700 ps, and the resolution on t_p was about 200 ns. Single QD emission intensity trajectories were generated by binning photons according to t_p, allowing τ_p to be studied as a function of either intensity or t_p. The PL decay data were fit to decay functions in Matlab using the Nelder−Mead Simplex minimization algorithm.

Results

Examples of typical TCSPC-generated PL decays from single QDs are shown in Figure 1. These PL decays were obtained by conventional TCSPC and will be referred to as "time-averaged" PL decays, to contrast them with "maximum-intensity" decays, which use only some of the photons collected by TTTR measurements as discussed later.

The PL decay for all QDs investigated fluctuated during the course of the TTTR measurement. Figure 2a shows this phenomenon explicitly by plotting the PL decay for 1-s TCSPC integration bins, over the 120 s of collection for this particular QD. Figure 2b shows the emission intensity trajectory for the dot in Figure 2a, plotted using 100-ms bins. Figure 2c shows more explicitly how the lifetime varies with the emission intensity by plotting three different PL decays that were generated by photons collected during short (1 s) periods of low, medium, and high count rates. Figures 2d and 2e show the method used to discriminate collected photons according to the emission intensity for the time bins from which they originate. For each single-dot TTTR measurement, an intensity trajectory was generated by binning photons with absolute arrival times (t_p) into 100-ms bins. Intensity thresholds were set at 10, 60, and 90% of the difference between the maximum and minimum emission intensities ($I_{thresh} = I_{min} + (\%/100)(I_{max} - I_{min})$). All photons were then categorized according to the emission-intensity range of their time bin. Separate single photon counting PL decay histograms were generated for each intensity range as shown in Figure 2e. The PL decays generated by photons from bins with emission intensity > 90% are referred to as "maximum-intensity" PL decays, in contrast to the time-averaged PL decays shown in Figure 1 that used all of the photons.

The results of fitting our data to a stretched exponential decay model

$$y(t) = c + a \exp(-(t/\tau)^{\beta}) \quad (1)$$

are shown in Figure 3 where the distribution of β values over 180 selected single QD measurements is displayed for the maximum-intensity PL decays (black) vs the time-averaged PL decays (gray). The distributions shown here were fitted to a log-normal distribution.

Figure 4a shows the distribution of single-exponential fits to the maximum-intensity PL decays for the three different samples used. The mean maximum-intensity lifetimes for samples 1, 2, and 3 were 26.5, 24.6, and 24.6 ns respectively. The inset to Figure 4a shows the overall distribution of lifetimes for all QDs considered. The mean maximum-intensity lifetime for these 122 QDs was 25.0 ns. The 1/e lifetime for time-averaged PL decays was much shorter and less consistent. Figure 4b shows two pairs of PL decays. Each pair represents two successive measurements on the same QD. The left panel shows two successive maximum-intensity PL decays, while the right panel shows the pair of time-averaged PL decays taken from the same TTTR measurements.

Figure 5 plots the integrated area beneath the intensity-normalized PL decay curves for a single QD as a function of its emission intensity. The error bars display the emission-intensity range of the bins used. These ranges were defined for this figure by thresholds of 10, 40, 60, and 90%. The symbols (●) in the plot represent the average intensity for that range. A linear relationship as in Figure 5 is found for nearly all of the QDs.

Discussion

The multiexponential time-averaged single-dot PL decays in Figure 1 explain the multiexponential behavior observed in ensemble samples, each individual QD exhibits multiexponential dynamics in the time-averaged PL decays (averaged for 120 s). The single-dot multiexponential behavior is caused by fluctuating lifetimes that are correlated to single-dot emission intensities,

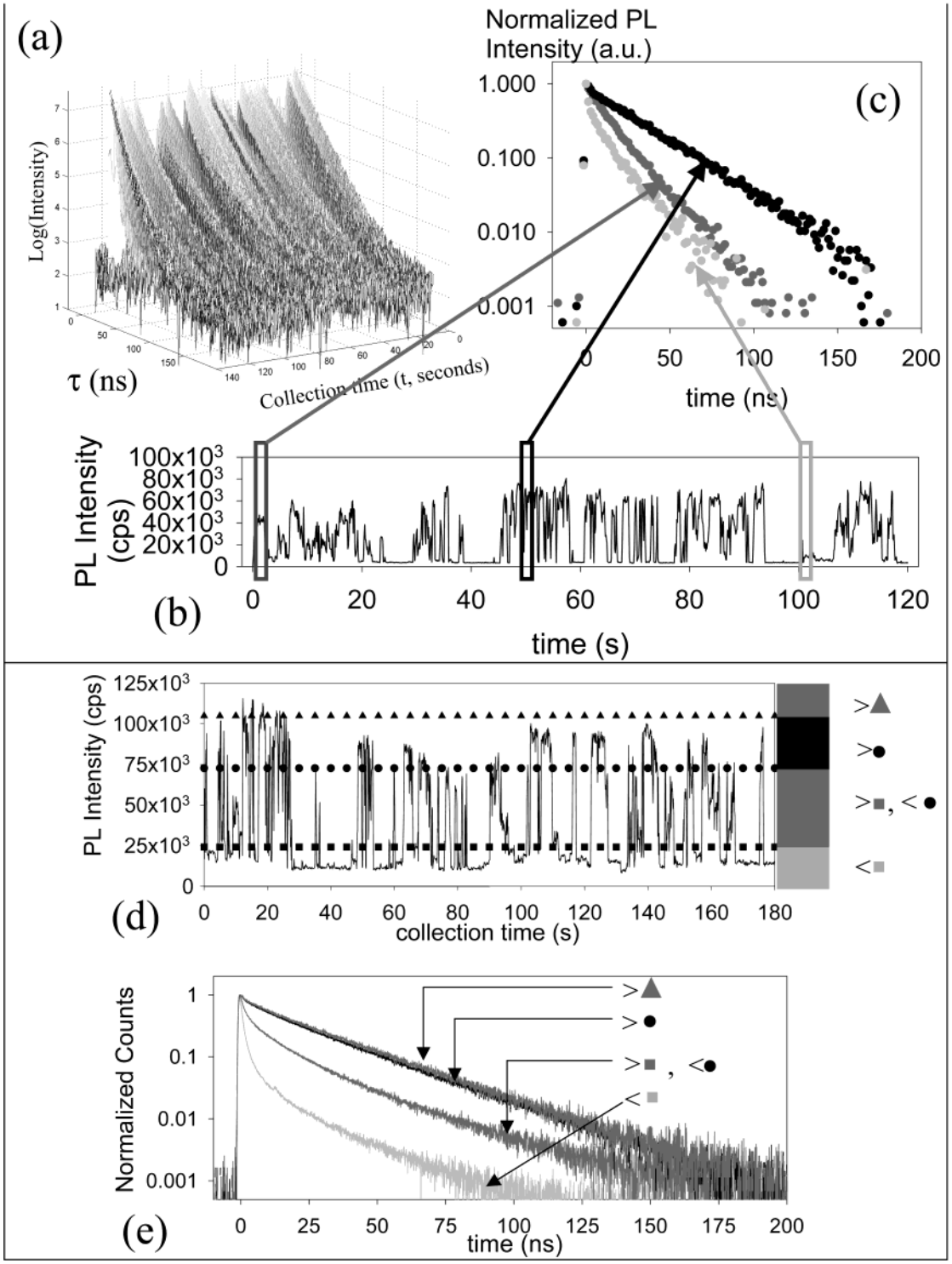

Figure 2. (a) Three-dimensional count intensity vs stochastic photon arrival time (start−stop time in nanoseconds) and collection time (in seconds). The intensity is plotted on a logarithmic scale. (b) Emission-intensity trajectory for the data in 2a. (c) Three different PL decays result from photons collected during different short periods of low (light gray), medium (dark gray), and high (black) emission intensities of the trajectory in 2c. (d) Emission-intensity trajectory from single QD with four intensity ranges defined by the three threshold levels of 10 (■), 60 (●), and 90% (▲). (e) PL decay curves generated by using only photons from time bins of 2d whose emission intensity falls within one of the four ranges shown. For instance, the black PL decay is generated only by photons from bins whose average emission intensity was above the 60% line (●) and below the 90% line (▲) in 2d.

as shown in Figure 2. The increase in lifetimes with higher emission intensities strongly suggests that fluctuations in the nonradiative rate (k_{nr}) are dominant. If fluctuations of the radiative rate were dominant, a decreased lifetime would correspond to an increased quantum yield (QY) and increased PL intensity. Surface and other external trap states provide a source of nonradiative relaxation pathways for single excitons in colloidal QDs.[5] However carrier trapping into QD surface states usually occurs on sub-nanosecond time scales. The fluctuating lifetimes instead must reflect fluctuations in coupling of the QD excited state to nonradiative trap states that are further away from the QD core's surface.

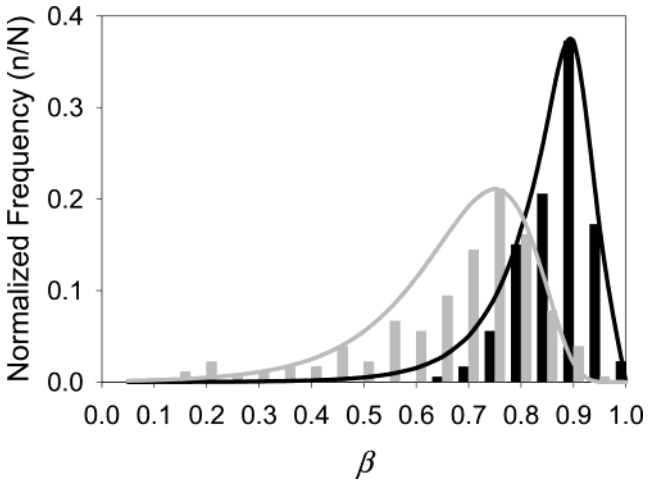

Figure 3. Distribution of stretched exponential (eq 1) β parameters when fitting the maximum-intensity PL decay (black) to the time-averaged PL decay (gray). The average β value for the maximum-intensity PL decays was 0.90, whereas the average β value for the corresponding time-averaged PL decays was 0.75. Log-normal fits to these two β distributions are superimposed for comparison.

Besides having longer time constants, the maximum-intensity PL decays are also nearly single exponential. The single-exponential character of these PL decays is apparent in Figure 2. Fitting the maximum-intensity PL decays to stretched exponentials (eq 1) quantifies, through the parameter β, how closely the maximum-intensity PL decay approaches single-exponential kinetics. Pure single-exponential behavior has $\beta = 1$, whereas smaller β values reflect a distribution of decay rates leading to greater multiexponential character.[13] The distribution of β values shown in Figure 3 quantitatively demonstrates the degree to which the maximum-intensity PL decay approaches single-exponential behavior, in contrast to the time-averaged, standard TCSPC measurement generated from the same TTTR measurements. Over 90% of the maximum-intensity PL decays have stretched exponential β parameters greater than 0.8 while more than 70% of the time-averaged PL decays have $\beta < 0.8$.

The hypothesis that k_{nr} for the single QD is fluctuating between various values is supported by the fact that whereas the maximum-intensity PL decay is nearly single exponential, PL decays generated from a narrow range of medium intensity data over the entire TTTR measurement are invariably multi-exponential. On the other hand, if data from the same medium-intensity range but limited to a short time span (e.g., a few seconds) is used to generate the PL decay, nearly single-exponential character (with a shorter lifetime) can again be recovered. An instance of this can be seen by comparing the medium-intensity PL decay of Figure 2e (integrated over the entire TTTR measurement) against the more single-exponential medium-intensity PL decays shown in Figure 2c (data taken from only a few seconds of the TTTR measurement).

The appearance of single-exponential character for maximum-intensity PL decays reveals an intrinsic property of the QD core that is independent of its surface cap or local environment, factors that dominate most other single QD measurements. Single-exponential kinetics results from a single rate constant, $k = k_r + k_{nr}$, where k_r is the rate of radiative transition and k_{nr} is the sum of all (varying) nonradiative rates. Given the

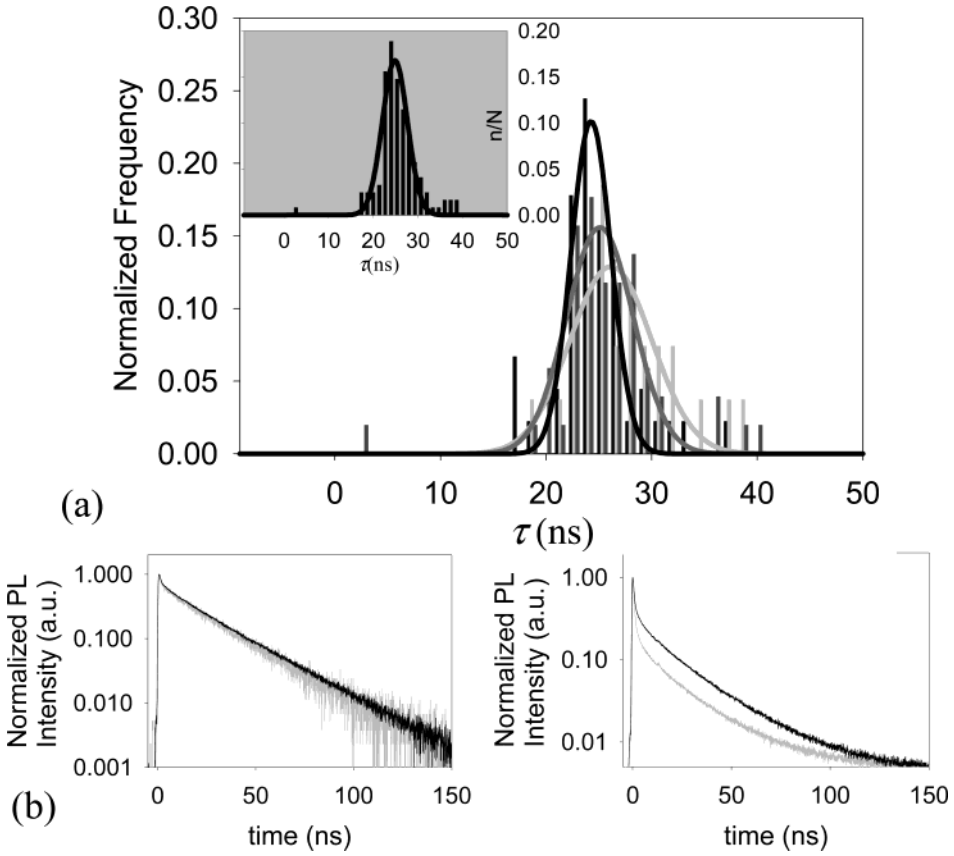

Figure 4. (a) Normalized distribution of single-exponential lifetime (τ) values from QDs with stretched exponential $\beta > 0.85$ for each of the three samples along with fits to the normal distribution. The mean lifetimes for samples 1 (gray), 2 (dark gray), and 3 (black) were 26.5, 24.6, and 24.6 ns, respectively. The inset of 4a displays the normalized distribution for all of the QDs taken together along with a Gaussian fit. The overall mean lifetime is 25.0 ns. (b) Two consecutive PL decay measurements from the same QD. On the left, the maximum-intensity PL decays for the two consecutive measurements are shown. On the right are the time-averaged PL decays for these same measurements.

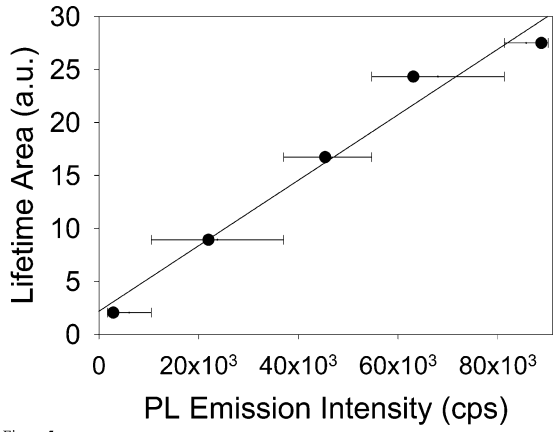

Figure 5. The average emission intensity for a particular intensity range of the trajectory is compared to the area beneath the normalized PL decay curve that is generated by photons from bins whose intensity falls in that range. The error bars indicate the range of emission-intensity values for the photons used to generate the PL decay whose area is calculated. The linear relationship between emission intensity and PL decay area indicates that the variations of emission intensity can be attributed to QY fluctuations.

fluctuating environment of the QY, it is unlikely that the same nonradiative pathway (i.e., same k_{nr}) will be repeatedly visited over a collection period of two or three minutes. It is more probable that the single-exponential decay measured from the maximum intensity photons is dominated by k_r, the radiative lifetime of the single QD. That is, $k_{max} \sim k_r$ (max = maximum intensity).

The hypothesis that the maximum-intensity PL decay measures the room-temperature radiative lifetime (τ_r) for the QD is suggested by the robustness of the measured lifetime value when fit to a single exponential, as shown in Figure 4a. These data show that the value of the maximum-intensity lifetime is nearly constant across all QDs, even for dots originating from different samples. Furthermore, the percent standard deviation of maximum-intensity lifetimes about the mean is much less than the percent standard deviation of the corresponding ($1/e$) times for time-averaged PL decays taken from the same QDs. In Figure 4b, sequential lifetime measurements on the same QD show that the maximum-intensity PL decay was reproducible unlike the time-averaged PL decay. We expect the radiative lifetime to remain essentially constant from measurement to measurement, whereas the time-averaged PL decay integrates all of the varying, environmentally influenced nonradiative components of the lifetime, making it less reproducible in sequential measurements. While the arguments above support our speculation that it is the radiative lifetime that is being measured, a direct measurement of the QY at the single QD level is required to absolutely confirm our hypothesis. This difficult measurement is beyond the scope of this work at this time.

The observed emission intensity dependence of single QD lifetimes coupled with the hypothesis that the maximum-intensity lifetime approaches a constant value (k_{max}^{-1}) with single-exponential character leads to an important modification of our understanding of the emission-intensity trajectories observed from single QDs: the intensity trajectory is determined not by digital intermittency alone but also by a fluctuating QY of the on state. Conventional wisdom says that fluorescence intermittency or blinking determines fluctuations in the intensity trajectory from a single QD. Numerous studies[2,3,14,15] have helped establish a model mechanism for this blinking wherein a QD switches between on and off states via charging events. Charging events turn the QD from on to off (off to on) by opening (closing) highly efficient Auger nonradiative recombination channels. Because the Auger recombination channel has a rate that is orders of magnitude faster than competing processes,[16−18] digital behavior is predicted, either the dot is on with some constant intensity or it is completely off.[14] Deviations from perfect digital behavior have been attributed to the finite time resolution of the measurement.

Since the time scale of intermittency has been shown to span up to five decades in time with event times extending down to 10 ms or less,[15] it is difficult to rule out fast blinking as a source of medium-intensity data points in the intensity trajectory. We explored the possibility that the intermediate PL decays observed for medium intensity events could result from fast blinking and that its PL decay would be given by a simple superposition of long lifetime and short lifetime weighted by the amount of time the dot was on and off during each bin. We found that the actual PL decay observed for medium intensity events was almost never reproduced by simply calculating the weighted average of maximum-intensity and off-time PL decays. Moreover, since the maximum intensity lifetime tends to be constant and single exponential, perfect digital blinking of the QD should lead to a perfect equivalence between the time-averaged PL decay and the maximum-intensity PL decay. This is also not observed. Therefore we are convinced that, while fast blinking probably still causes some artificially low intensity points in the intensity trajectory, fluctuations in the nonradiative relaxation rate (k_{nr}) dominate intensity fluctuations in a single QD emission intensity trajectory.

Changes in k_{nr} imply that the "instantaneous QY" (i.e., the instantaneous probability of radiative rather than nonradiative relaxation) is fluctuating. We can relate the fluctuating PL decays to the fluctuating instantaneous QY though the integrated area beneath the intensity-normalized PL decay curve (A_N). A_N is a generalization of the single-exponential decay constant, τ, for cases of multiexponential decays, $Q = k_r\tau \rightarrow Q = k_rA_N$. This relationship is based on the definition of QY as the number of photons emitted (n_e) per number of photons absorbed (n_a), that is, $QY = n_e/n_a$. Since the number n_e is directly proportional to the area beneath the normalized PL decay curve, it follows that the QY is directly proportional to this PL decay area, assuming constant n_a, collection efficiency, etc.

Figure 5 explicitly shows the correlation between emission intensity and instantaneous QY. The observed emission intensity in a given range is related to A_N for the PL decay curve that was generated by photons arriving at times (t_p) with that emission intensity in that range. The linear relationship observed in Figure 5 indicates, therefore, that the emission intensity varies as a result of QY fluctuations that arise from changing nonradiative relaxation pathways. In other words, the observed intensity trajectory is dictated not only by purely digital intermittency between charged and uncharged states but also by a fluctuating QY of the emitting state.

We have presented data that demonstrate the emission-intensity dependence of PL decay measurements from single colloidal QDs. We have seen that the maximum-intensity PL decays approach single-exponential behavior, and their lifetimes are nearly constant from QD to QD and even from sample to sample. These observations lead us to speculate on the possibility that the maximum-intensity lifetime is actually the radiative lifetime. Furthermore, these results highlight the important role that QY fluctuations play in determining the intensity trajectory from single QDs.

Acknowledgment. B.R.F. acknowledges invaluable discussion and experimental advice from Jean-Michel Caruge as well as financial support from the NDSEG Fellowship program. This research was funded in part through the NSF MRSEC program at MIT (DMR-0213282), by the NSF funded Harrison Spectroscopy Laboratory (NSF-011370-CHE), by the Packard Foundation, and by the Department of Energy (DE-DFG02-02ER45974).

Supporting Information Available: Synthesis of nanocrystallites. This material is available free of charge via the Internet at http://pubs.acs.org.

References and Notes

(1) Empedocles, S. A.; Norris, D. J.; Bawendi, M. G. Photoluminescence Spectroscopy of Single CdSe Nanocrystallite Quantum Dots. *Phys. Rev. Lett.* **1996**, *77*, 3873.

(2) Kuno, M., et al. Nonexponential "blinking" kinetics of single CdSe quantum dots: A universal power law behavior. *J. Chem. Phys.* **2000**, *112*, 3117.

(3) Shimizu, K. T., et al. Blinking Statistics in Single Semiconductor Nanocrystal Quantum Dots. *Phys. Rev. B* **2001**, *63*, 205316.

(4) Empedocles, S. A.; Bawendi, M. G. Influence of Spectral Diffusion on the Line Shapes of Single CdSe Nanocrystallite Quantum Dots. *J. Phys. Chem. B* **1999**, *103*, 1826−1830.

(5) Bawendi, M. G., et al. Luminescence Properties of CdSe quantum crystallites: Resonance between interior and surface localized states. *J. Chem. Phys.* **1991**, *96*, 946.

(6) Schlegel, G., et al. Fluorescence Decay Time of Single Semiconductor Nanocrystals. *Phys. Rev. Lett*. **2002**, *88*, 137401.

(7) Edman, L.; Ulo, M.; Rigler, R. Conformational transitons monitored for single molecules in solution. *Proc. Natl. Acad. Sci., U. S. A.* **1996**, *93*, 6710−6715.

(8) Geva, E. A.; Skinner, J. L. Two-state dynamics of single biomolecules in solution. *Chem. Phys. Lett.* **1998**, *288*, 225−229.

(9) Neuhauser, R. G., et al. Correlation between Fluorescence Intermittency and Spectral Diffustion in Single Semiconductor Quantum Dots. *Phys. Rev. Lett.* **2000**, *85*, 3301.

(10) Ebenstein, Y.; Mokari, T.; Banin, U. Fluoresecence quantum yield of CdSe/ZnS nanocrystals investigated by correlated atomic-force and single-particle fluorescence microscopy. *Appl. Phys. Lett.* **2002**, *80*, 4033−4035.

(11) Bawendi, M. G.; Stott, N. E. Preparation of nanocrystallites. U.S. Patent 6,576,291, 2003.

(12) Dabbousi, B. O., et al. (CdSe)ZnS Core−Shell Quantum Dots: Synthesis and Characterization of a Size Series of Highly Luminescent Nanocrystallites. *J. Phys. Chem. B* **1997**, *101*, 9463−9475.

(13) Lindsey, C. P.; Patterson, G. D. Detailed Comparison of the Williams-Watts and Cole−Davidson Functions. *J. Chem. Phys.* **1980**, *73*, 3348.

(14) Efros, A. L. Random Telegraph Signal in the Photoluminescence Intensity of Single Quantum Dot. *Phys. Rev. Lett.* **1997**, *78*, 1110.

(15) Kuno, M., et al. "On"/"off" fluorescence intermittency of single semiconductor quantum dots. *J. Chem. Phys.* **2001**, *115*, 1028.

(16) Klimov, V. I.; McBranch, D. W. Auger-process-induced charge separation in semiconductor nanocrystals. *Phys. Rev. B* **1997**, *55*(19), 13173−13179.

(17) Klimov, V. I. Optical nonlinearities and ultrafast carrier dynamics in semiconductor nanocrystals. *J. Phys. Chem. B* **2000**, *104*, 6112−6123.

(18) Efros, A. L. Auger Processes in Nanosize Semiconductor Crystals. In *Archives* 2002, Naval Research Laboratory, 2002.